How Can Proteins Enter the Interior of a MOF? Investigation of Cytochrome *c* Translocation into a MOF Consisting of Mesoporous Cages with Microporous Windows

Yao Chen, Vasiliki Lykourinou, Carissa Vetromile, Tran Hoang, Li-June Ming, Randy W. Larsen, and Shengqian Ma*

Department of Chemistry, University of South Florida, 4202 East Fowler Avenue, Tampa, Florida 33620, United States

S *Supporting Information*

ABSTRACT: It has been demonstrated for the first time that the heme protein cytochrome *c* (Cyt *c*) can enter the interior of a MOF despite the larger molecular dimension of the protein relative to the access pore sizes. Mechanistic studies suggest that the Cyt *c* molecules must undergo a significant conformational change during translocation into the MOF interior through the relatively small nanopores.

Protein transport is an essential mechanism in living cells.[1] For protein translocation into organelles such as mitochondria,[2] the endoplasmic reticulum,[3] and chloroplasts,[4] the proteins are typically transported through protein-conducting channels comprising nanopores smaller than the dimensions of the protein.[5] Thus, in order for the protein to enter the organelle, it must undergo significant conformational changes during the translocation process.[6] The biological mechanism associated with protein transport through membranes suggests a mechanism through which proteins could also be transported through porous solid-state materials,[7] including metal–organic frameworks (MOFs), a new class of functional materials with uniform nanopores.

MOFs are highly crystalline inorganic–organic hybrids that are constructed by assembling metal ions or metal-containing clusters with multidentate organic ligands via coordinate bonds.[8] These materials feature structural diversity and amenability to be designed with specific functionality.[9] Their tunable but uniform pore sizes and functionalizable pore walls allow the available nanospace to accommodate a variety of guest species for applications in gas storage/separation,[10] catalysis,[11] sensing,[12] drug delivery,[13] etc. A relatively unexplored aspect of MOF-based materials is their potential to utilize the associated nanopores to encapsulate large biomolecules.[14] Encapsulation of biomolecules into MOF nanopores postsynthetically would require a protein transport process similar to that utilized for import into cellular organelles. Thus, MOFs provide an exciting opportunity to probe the mechanistic details of protein pore migration.

We recently demonstrated the successful immobilization of microperoxidase-11 (MP-11) into a MOF.[15] Although MP-11 is a "microenzyme" with relatively small molecular dimensions, this study provided a proof of concept for the immobilization of larger proteins into the interior of a MOF. In this contribution, we report the encapsulation of the heme protein cytochrome *c*

(Cyt *c*) in a nanoporous MOF despite the much larger molecular dimension of the protein relative to the pore sizes of the MOF. The data presented further indicate that the Cyt *c* molecules enter the MOF through the narrow nanopores by undergoing conformational changes, reminiscent of the process of protein translocation into some organelles via small nanopores.

Cyt *c* is a relatively small, structurally robust heme protein with molecular dimensions of ~2.6 nm × 3.2 nm × 3.3 nm that serves as a component of the electron transport chain in mitochondria and is involved as a signal associated with apoptosis.[16] The protein consists of a single polypeptide chain of 104 amino acid residues containing a covalently attached heme group (Figure 1).[17] In view of the stability of its


Figure 1. Molecular structure of cytochrome *c* (PDB entry 1OCD).

framework in buffer solutions, the MOF known as Tb-mesoMOF provides an excellent platform for investigating the interaction between Cyt *c* and MOF nanopores. Tb-mesoMOF is based upon triazine-1,3,5-tribenzoate (TATB) ligands (Figure 2a) that link Tb_4 moieties to form truncated supertetrahedrons (STs) (Figure 2b). The truncated STs are extended by TATB ligands to form a three-dimensional network with the MTN topology (Figure 2c) in which two types of nanoscopic cages exist: 3.9 nm diameter cages that are surrounded by 20 truncated STs and have 12 pentagonal windows (pink in Figure 2c) and 4.7 nm diameter cages that are defined by 28 truncated STs and have 12 pentagonal and 4 hexagonal windows (green in Figure 2c). These nanoscopic cages are interconnected through five- and six-membered-ring pores (windows), which, on the basis of the van der Waals radii,
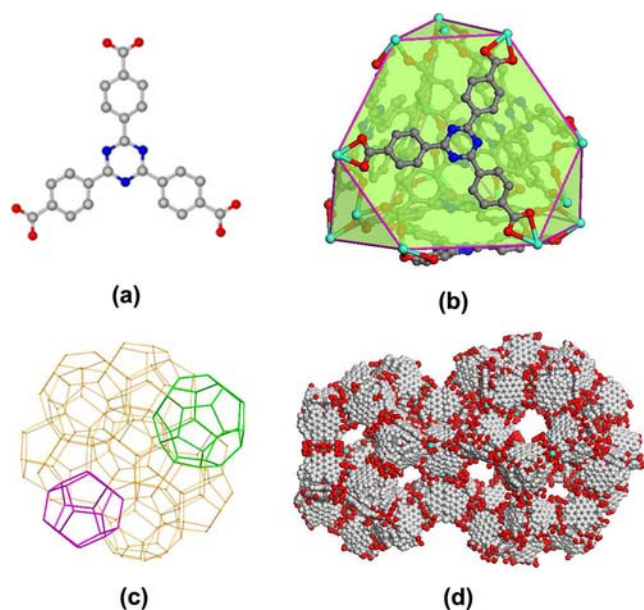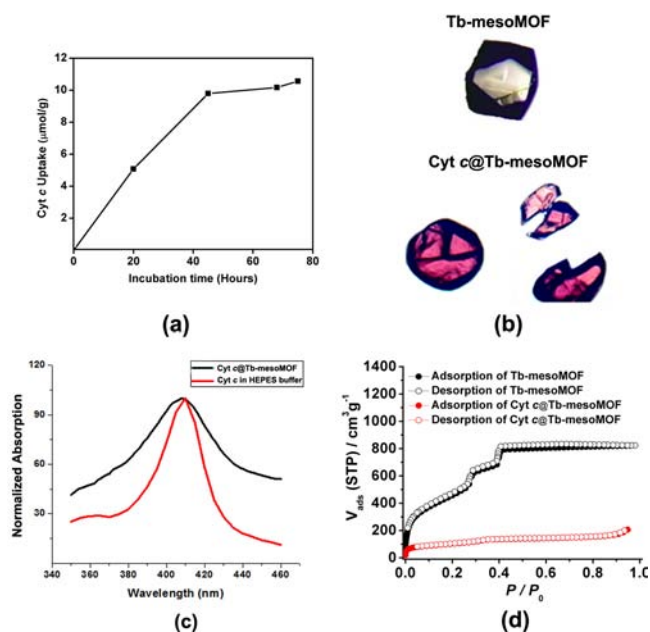
Figure 2. (a) TATB ligand. (b) Truncated supertetrahedron in Tb-mesoMOF. (c) MTN topology of Tb-mesoMOF. The two types of cages are highlighted in green and pink. (d) A 3.9 nm diameter cage and a 4.7 nm diameter cage interconnected through 1.3 and 1.7 nm windows in Tb-mesoMOF. Color scheme: C, gray; O, red; N, blue; Tb, turquoise.


Figure 3. (a) Profile of Cyt *c* uptake by Tb-mesoMOF in HEPES buffer at 37 °C. (b) Optical images of (top) a Tb-mesoMOF crystal and (bottom) a Cyt *c*@Tb-mesoMOF crystal (left) before and (right) after fracturing. (c) UV−vis absorption spectra of Cyt *c*@Tb-mesoMOF (black) and free Cyt *c* in HEPES buffer solution (red). (d) N_2 sorption isotherms of Tb-mesoMOF (black) and Cyt *c*@Tb-mesoMOF (red).

have free diameters of 1.3 and 1.7 nm, respectively (Figure 2d).[18] In view of the dimensions of the Cyt *c* molecule as well as the hydrophobic property of the Tb-mesoMOF framework, Cyt *c* import into the MOF interior would require the protein to undergo a change in conformation initiated first by surface contacts between the protein and the MOF crystal. Migration of the protein through the relatively small nanopores to enter the 3.9 and 4.7 nm diameter cages would require a partial unfolding of the protein's tertiary structure.

To explore the possibility of Cyt *c* immobilization within Tb-mesoMOF, freshly prepared Tb-mesoMOF crystals were immersed in a solution of bovine heart Cyt *c* solubilized in 4-(2-hydroxyethyl)-1-piperazineethanesulfonic acid (HEPES) buffer, and the solution was placed in an incubator at 37 °C. The uptake of Cyt *c* by Tb-mesoMOF at different time points was determined using the bicinchoninic acid (BCA) method for protein determination.[19] As shown in Figure 3a, a saturated loading of ~10.2 µmol/g was reached after ~45 h. The Cyt *c*/Tb-mesoMOF sample (hereafter denoted as Cyt *c*@Tb-mesoMOF) was then washed with fresh buffer solution until the supernatant became colorless to fully remove loosely bound Cyt *c* molecules. Inductively coupled plasma mass spectrometry (ICP-MS) and atomic absorption (AA) studies on the washed Cyt *c*@Tb-mesoMOF sample revealed a Cyt *c* uptake ~9.8 µmol/g, in good agreement with the loading amount determined by the BCA method. The successful immobilization of Cyt *c* into Tb-mesoMOF was confirmed by crystal optical images and UV−vis spectroscopy. The Tb-mesoMOF crystals became distinctly colored after being saturated with Cyt *c* (Figure 3b), strongly indicating the association of Cyt *c* molecules with Tb-mesoMOF. Solid-state UV−vis absorption spectroscopy studies revealed that Cyt *c*@Tb-mesoMOF exhibited a Soret band at ~410 nm, which is consistent with the Soret band of ~411 nm for Cyt *c* in buffer solution (Figure 3c). Fracturing the crystal revealed that the crystal interior also

displayed optical images retaining the color of the heme macrocycle (Figure 3b), indicating diffusion of Cyt *c* molecules into the interior pores of the Tb-mesoMOF crystal. As the heme is covalently attached to the protein, any indication of the presence of heme also indicates the protein is present as well. N_2 sorption isotherms (Figure 3d) measured at 77 K indicated that the Brunauer−Emmett−Teller (BET) surface area of Tb-mesoMOF decreased from 1935 to 348 m^2/g after association with Cyt *c*, further supporting the successful immobilzation of Cyt *c* into the interior cavities of Tb-mesoMOF. Tb-mesoMOF retained its framework integrity after encapsulation of Cyt *c*, as evidenced by powder X-ray diffraction (PXRD) studies (Figure S1).

The successful immobilization of Cyt *c* into the interior of the Tb-mesoMOF can only take place if the protein undergoes a conformational change that reduces the overall dimensions of the protein, allowing migration through the open pores at the crystal surface. Steady-state fluorescence spectroscopy provides a convenient method for determining conformational changes within a protein.[20] In the case of Cyt *c*, the polypeptide chain contains a single tryptophan residue (Trp59) and four tyrosine residues (Tyr48, -67, -74, and -97) that contribute to the fluorescence spectrum of the protein.[21] The Trp59 residue is located ~5 Å from the heme edge, and the emission is highly quenched in the folded protein.

The steady-state fluorescence spectra of Cyt *c* in buffer solution (50 mM phosphate, pH 7.5), Cyt *c* in buffer containing 6 M guanidine HCl (GdnHCl), and Cyt *c*@Tb-mesoMOF are displayed in Figure 4a. As discussed above, the spectrum of Cyt *c* in buffer was nearly completely quenched by the heme group. Upon unfolding of the protein in GdnHCl, emission maxima centered at 303 and 353 nm (with nearly equal intensity) were observed, corresponding to solvent-exposed Tyr and Trp
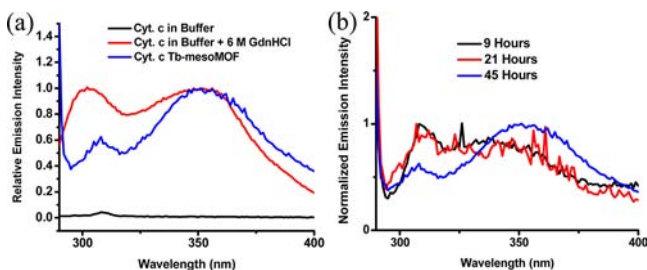
Figure 4. Fluorescence spectra of (a) Cyt *c* in HEPES buffer, Cyt *c* denatured by GdnHCl, and Cyt *c*@Tb-mesoMOF and of (b) Cyt *c*@ Tb-mesoMOF after different incubation times.

residues, respectively, that are much farther from the heme group. Interestingly, Cyt *c*@Tb-mesoMOF displayed an emission spectrum with a maximum at ~353 nm and a lower-intensity band centered at ~307 nm ($I_{303 nm}/I_{353 nm} = 1$ for Cyt *c* in GdnHCl and 0.6 for Cyt *c*@Tb-mesoMOF). These results indicate that the protein located within the Tb-mesoMOF interior exists in a non-native conformation that is distinct from that of the GdnHCl-unfolded protein.

Figure 4b displays the progression of fluorescence changes associated with confinement of Cyt *c* within Tb-mesoMOF. At early times, the fluorescence spectra resemble that of the GdnHCl-denatured protein but with a progressively red-shifted Trp fluorescence maximum. These data support a mechanism for Cyt *c* translocation into Tb-mesoMOF (Scheme 1) in which

Scheme 1. Tentative Mechanism for the Translocation of Cyt *c* into the Cavities of Tb-mesoMOF[a]
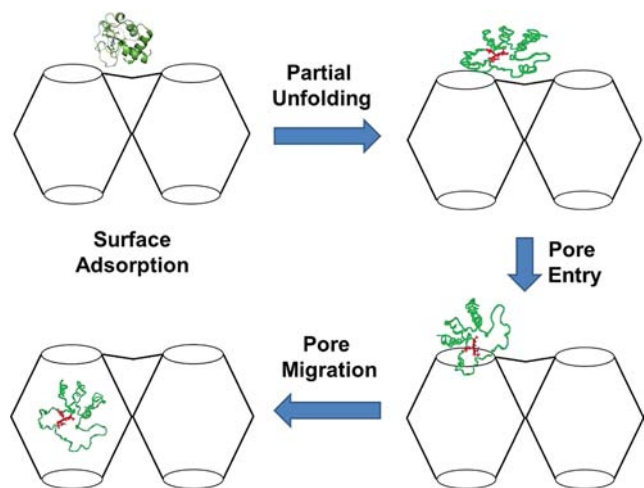
[a]The red coil represents the heme part of Cyt *c*. The mechanism involves surface adsorption of the protein (top left) followed by partial unfolding (top right); the partially unfolded protein is partitioned between the surface and exterior pores (bottom right) and then migrates into the large interior cavities (bottom left).

Cyt *c* molecules first adsorb onto the surface of the MOF crystals. Cyt *c* is known to undergo conformational perturbation upon binding to surfaces, resulting in cleavage of the Met80−Fe bond of the heme group and tertiary structure destabilization.[22−24] The partially unfolded protein (characterized by the Trp emission at ~345 nm) can adopt a size and an orientation that is more amenable to migration through the surface pore, leading to partitioning of the protein between the surface and the exterior nanopores (pore entry). At longer

incubation times, the protein continues to be partitioned into the interior cavities through the relatively small nanopores (pore migration) and is stabilized through the exposure of hydrophobic amino acids from the protein's interior to the hydrophobic interior of the Tb-mesoMOF cavities, resulting in a new protein conformation exhibiting a distinct fluorescence emission centered at ~353 nm. The position of the Trp emission is indicative of water exposure, suggesting that the protein entrapped within the Tb-mesoMOF cavities retains significant water content despite the hydrophobic nature of the interior cavities.[25] Furthermore, the color of the fractured Cyt *c*@Tb-mesoMOF crystals indicates that the encapsulated protein likely retains a six-coordinate low-spin heme *c* macrocycle.

In summary, we have demonstrated for the first time that the heme protein Cyt *c* can enter the interior cavities of a MOF with pore sizes that are small relative to the molecular dimensions of Cyt *c*. The results of fluorescence studies further have suggested that Cyt *c* undergoes conformational changes during the immobilization process and adopts a conformation that is distinct from either its native conformation or that of the GdnHCl-denatured protein. A protein transport mechanism that contains the salient features of protein translocation into cellular organelles has been proposed. This work lays a foundation for employing MOFs as a new class of platforms for protein translocation studies. Ongoing work in our laboratory includes investigations of the biocatalysis performance of Cyt *c*@Tb-mesoMOF and the processes of translocation of other protein molecules into porous MOFs.

■ ASSOCIATED CONTENT

ⓈSupporting Information

Experimental procedures for Cyt *c* uptake, fluorescence, ICP-MS, and AA experiments and figures showing PXRD patterns, TGA plots, and fluorescence spectra. This material is available free of charge via the Internet at http://pubs.acs.org.

■ AUTHOR INFORMATION

Corresponding Author
sqma@usf.edu

Notes
The authors declare no competing financial interest.

■ ACKNOWLEDGMENTS

■ REFERENCES

(1) Pfanner, N.; Geissler, A. *Nat. Rev. Mol. Cell Biol.* **2001**, *2*, 339.
(2) Marom, M.; Azem, A.; Mokranjac, D. *Biochim. Biophys. Acta* **2011**, *1808*, 990.
(3) Zimmermann, R.; Eyrisch, S.; Ahmad, M.; Helms, V. *Biochim. Biophys. Acta* **2011**, *1808*, 912.
(4) Li, H. M.; Chiu, C. C. *Annu. Rev. Plant Biol.* **2010**, *61*, 157.
(5) Rapoport, T. A. *Nature* **2007**, *450*, 663.
(6) Wickner, W.; Schekman, R. *Science* **2005**, *310*, 1452.

(7) (a) Hartmann, M.; Jung, D. *J. Mater. Chem.* **2010**, *20*, 844. (b) Hartmann, M. *Chem. Mater.* **2005**, *17*, 4577. (c) Hudson, S.; Cooney, J.; Magner, E. *Angew. Chem., Int. Ed.* **2008**, *47*, 8582.

(8) (a) Long, J. R.; Yaghi, O. M. *Chem. Soc. Rev.* **2009**, *38*, 1213. (b) Zhou, H.-C.; Long, J. R.; Yaghi, O. M. *Chem. Rev.* **2012**, *112*, 673.

(9) (a) Perry, J. J.; Perman, J. A.; Zaworotko, M. J. *Chem. Soc. Rev.* **2009**, *38*, 1400. (b) O'Keeffe, M.; Yaghi, O. M. *Chem. Rev.* **2012**, *112*, 675.

(10) (a) Ma, S.; Zhou, H.-C. *Chem. Commun.* **2010**, *46*, 44. (b) Suh, M. P.; Park, H. J.; Prasad, T. K.; Lim, D.-W. *Chem. Rev.* **2012**, *112*, 782. (c) Wu, H.; Gong, Q.; Olson, D. H.; Li, J. *Chem. Rev.* **2012**, *112*, 836. (d) Li, J.-R.; Sculley, J.; Zhou, H.-C. *Chem. Rev.* **2012**, *112*, 869. (e) Sumida, K.; Rogow, D. L.; Mason, J. A.; McDonald, T. M.; Bloch, E. D.; Herm, Z. R.; Bae, T.-H.; Long, J. R. *Chem. Rev.* **2012**, *112*, 724.

(11) (a) Lee, J.; Farha, O. K.; Roberts, J.; Scheidt, K. A.; Nguyen, S. T.; Hupp, J. T. *Chem. Soc. Rev.* **2009**, *38*, 1450. (b) Corma, A.; García, H.; Llabres i Xamena, F. X. *Chem. Rev.* **2010**, *110*, 4606. (c) Yoon, M.; Srirambalaji, R.; Kim, K. *Chem. Rev.* **2012**, *112*, 1196.

(12) (a) Kreno, L. E.; Leong, K.; Farha, O. K.; Allendorf, M.; Van Duyne, R. P.; Hupp, J. T. *Chem. Rev.* **2012**, *112*, 1105. (b) Cui, Y.; Yue, Y.; Qian, G.; Chen, B. *Chem. Rev.* **2012**, *112*, 1126.

(13) Horcajada, P.; Gref, R.; Baati, T.; Allan, P. K.; Maurin, G.; Couvreur, P.; Férey, G.; Morris, R. E.; Serre, C. *Chem. Rev.* **2012**, *112*, 1232.

(14) (a) Chen, Y.; Lykourinou, V.; Hoang, T.; Ming, L.-J.; Ma, S. *Prepr. Symp.—Am. Chem. Soc., Div. Fuel Chem.* **2012**, *57*, 1000. (b) Deng, H.; Grunder, S.; Cordova, K. E.; Valente, C.; Furukawa, H.; Hmadeh, M.; Gandara, F.; Whalley, A. C.; Liu, Z.; Asahina, S.; Kazumori, H.; O'Keeffe, M.; Terasaki, O.; Stoddart, J. F.; Yaghi, O. M. *Science* **2012**, *336*, 1018.

(15) Lykourinou, V.; Chen, Y.; Wang, X.-S.; Meng, L.; Hoang, T.; Ming, L.-J.; Musselman, R. L.; Ma, S. *J. Am. Chem. Soc.* **2011**, *133*, 10382.

(16) Harbury, H. A.; Loach, P. A. *J. Biol. Chem.* **1960**, *235*, 3640.

(17) Senn, H.; Wüthrich, K. *Q. Rev. Biophys.* **1985**, *18*, 111.

(18) Park, Y. K.; Choi, S. B.; Kim, H.; Kim, K.; Won, B.-H.; Choi, K.; Choi, J.-S.; Ahn, W.-S.; Won, N.; Kim, S.; Jung, D. H.; Choi, S.-H.; Kim, G.-H.; Cha, S.-S.; Jhon, Y. H.; Yang, J. K.; Kim, J. *Angew. Chem., Int. Ed.* **2007**, *46*, 8230.

(19) Smith, P. K.; Krohn, R. I.; Hermanson, G. T.; Gartner, F. H.; Fujimoto, E. K.; Goeke, N. M.; Olson, B. J.; Klenk, D. C. *Anal. Biochem.* **1985**, *150*, 76.

(20) Righetti, P. G.; Verzola, B. *Electrophoresis* **2001**, *22*, 2359.

(21) Pajot, P. *Eur. J. Biochem.* **1976**, *63*, 263.

(22) Pinheiro, T. J. T.; Elove, G. A.; Watts, A.; Roder, H. *Biochemistry* **1997**, *36*, 13122.

(23) Hildebrandt, P.; Stockburger, M. *Biochemistry* **1989**, *28*, 6722.

(24) Gong, J.; Yao, P.; Duan, H.; Jiang, M.; Gu, S.; Chunyu, L. *Biomacromolecules* **2003**, *4*, 1293.

(25) Vivian, J. T.; Callis, P. R. *Biophys. J.* **2001**, *80*, 2093.